Non-local damage modeling of high performance concrete exposed to high temperature

L. Ferrara & R. Felicetti
Department of Structural Engineering, Politecnico di Milano, Italy.

ABSTRACT: In this work the whole set of residual tensile properties have been assessed, in the framework of a non-local damage approach, for a high performance siliceous concrete (f_c = 72 MPa) at significant thermal damage levels (20, 250 and 400 °C). The basic idea is that the same concrete, after being exposed to high temperature, can be simply modeled as a different homogeneous material, the mechanical properties of which include all the effects of the undergone thermal damage. A major role is played by the material characteristic length, which takes into account the increasing material heterogeneity, and which has been experimentally identified through cross examination of direct tension tests on notched cylinders and PIED tests. A final check on a small scale structure has been performed with reference to an unreinforced deep beam (span/depth ratio = 2)

Keywords: mode I fracture, high performance concrete, thermal damage, non-local damage, characteristic length

1 INTRODUCTION

The mechanical properties of concrete at high temperature (up to 800-1000°C) are well known, thanks to the many tests carried out since the Sixties and Seventies (RILEM, 1985). However, further research activity is being performed in order to cover new materials (high-performance concrete - Phan and Carino, 1998) and certain aspects related to material fracture properties.

As regards test modalities, many test results and documents show that the damage induced by exposure to high temperature is mostly irreversible and remains "frozen" in the concrete, even after cooling down to room temperature. For this reason the mechanical properties measured directly under sustained high temperature or after gradually cooling down to room temperature are usually comparable. For instance, the residual compressive strength at room temperature is close to 85-90% of the “hot” strength and similar ratios have been found for the tensile strength (RILEM, 1985, Felicetti et al., 2000). On the contrary, tests at room temperature are far simpler to be conducted, especially when fracture properties are of concern and both an accurate control of the test and a close inspection of the results are needed.

Bearing this in mind, an extensive series of residual tests have been performed over the past years at Politecnico di Milano, in the framework of a research program on the mechanical properties of two high performance highly siliceous concretes (f_c = 72-95 MPa - Table 1) after exposure to slow thermal cycles (T_{max} = 20, 105, 250, 400, 500°C - temperature rate = 0.2°C/min). These results will be briefly recalled, in order to cast the base for the later discussion on the numerical modeling.

With reference to compression an astonishing decrease of both the residual strength and the Young's modulus have been observed after the exposure to temperatures higher than 250°C (Fig. 1 - Felicetti and Gambarova, 1998a). The very temperature sensitive flint-based aggregate is the main reason why these concretes proved to be really prone to thermal damage. One first consequence of this feature is that the two grades of concrete behave in almost the same way beyond 250°C. For this reason, reference will be made only to the lower grade concrete hereinafter. The second outcome, is that these materials exhibit significant thermal damage levels already at T_{max} = 250 and 400°C, even being still able to bear load for practical purposes.

Table 1. Concrete mix- design

Components (kg/m³)	**f_c = 72 MPa**	f_c = 95 MPa
Portland cement	290	415
Silica fume	30 (9.4%)	30 (6.7%)
Calcareous filler	105	0
Aggregate: crushed flint (sand /gravel /pebbles)	831 / 287 / 752	
Water (water/binder ratio)	138 (43%)	133 (30%)
Superplasticizer: (melammino-sulfonate)	10.6 (3.3%)	14.8 (3.3%)
Retarder	1.7 (0.5%)	2.4 (0.5%)
Slump (mm)	230	210

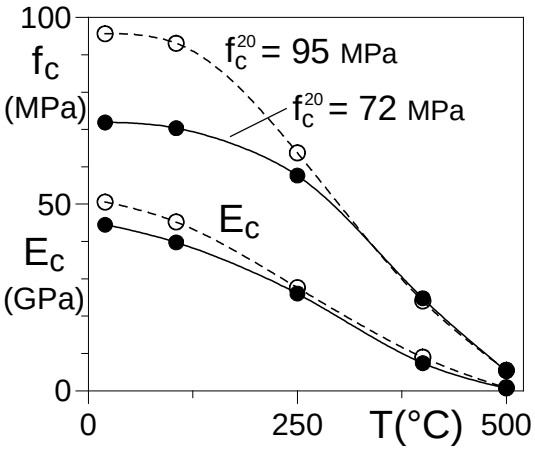

Figure 1. Residual compressive strength and Young's modulus for the concretes herein reported.

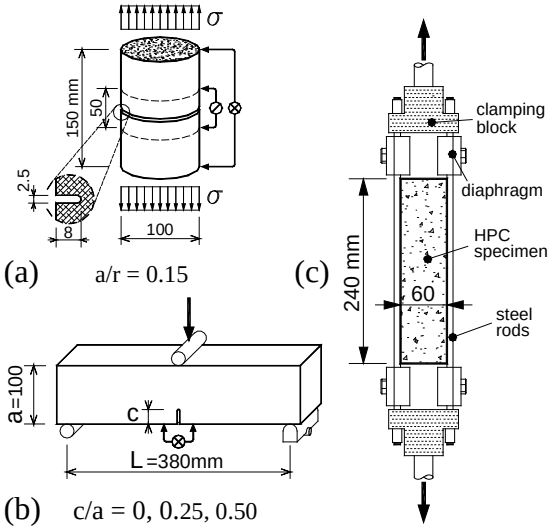

Figure 2. Specimen geometry for a) fixed-end direct-tension tests, b) three-point bending tests and c) PIED tests.

Thus, these two reference temperatures will be considered for modeling the response of the damaged specimens.

A deeper insight into the mechanical behavior of these uniformly pre-damaged concretes is allowed by the tests on notched cylinders in direct-tension and on unnotched and notched prisms in three point bending (Figure 2a, b - Felicetti and Gambarova, 1998b). Testing in direct tension is, in principle, the most suitable way to characterize the behavior of concrete in tension and to work out the values of such fundamental parameters as peak strength, fracture energy, critical crack width and slope of the falling branch. Nevertheless, both the heterogeneity and the softening behavior of concrete unavoidably introduce some "structural" effects if specimen ends are allowed to rotate (i.e. crack propagation and bending - Felicetti et al., 2000).

For this reason the fixed-end direct-tension technique has been adopted, allowing to average the material defects and to reduce the structural effects to a minimum. Due to the lack of structural effects, the direct-tensile strength turns out to be the most temperature sensitive mechanical parameter, whereas the strength decay in bending is partially shadowed by the gentler softening behavior of damaged concrete (Figure 3).

On the opposite edge is the case of a special tension test in which the crack localization is prevented by a number of metallic rods glued to the specimen sides (PIED tests - di Prisco et al., 1999). As a consequence, only a series of evenly distributed microcracks develops and the material can still be regarded as a uniformly stretched continuum. In the limited strain range permitted by this test ($\varepsilon < 1‰$) the comparison between the slope of the softening branch with either free or restrained localization allows to assess the material characteristic length h^I (Figure 4). According to Bazant's definition, this length can be regarded as the thickness of a blunt smeared crack band in which the material undergoes progressive microcracking at the onset of crack formation (on the rough assumption that the inelastic strain is uniform within the crack band).

The remarkable increase of the characteristic length with thermal damage effectively explains the limited influence of temperature on concrete fracture energy (Figure 5). At increasing thermal damage, larger volumes of weaker material are involved in the fracture process, yielding an almost constant energy dissipation upon crack propagation. Hence, the characteristic length is expected to play a key role for modeling the behavior of concrete structures submitted to fire, especially when the effect of strain gradients,

material defects and structural size are concerned.

The last remark ensuing from the results on fracture energy is that very similar values have been obtained in direct-tension and bending tests.

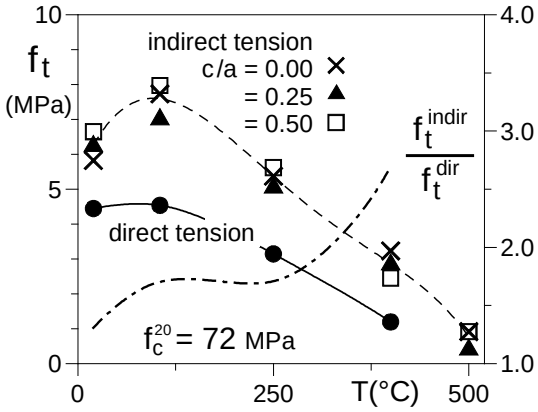

Figure 3. Residual direct-tension and bending strengths.

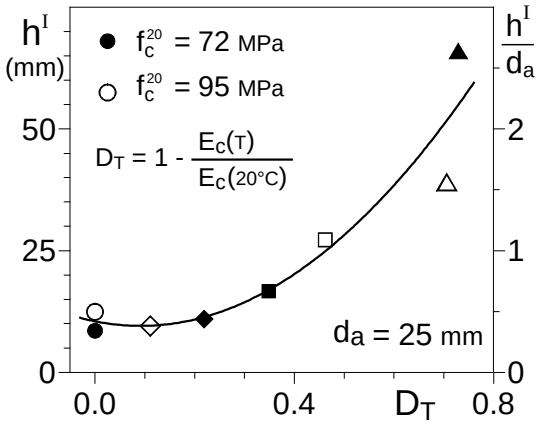

Figure 4. Characteristic length at increasing thermal damage.

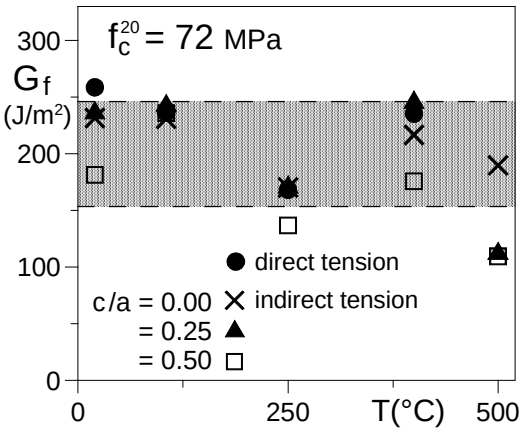

Figure 5. Total work of fracture in direct-tension (notched cylinders) and bending (notched and unnotched prisms).

The only exception are the most deeply notched beams (c/a=0.5), which exhibit a weaker response due to the limited ligament length and the sizable thermally induced pre-cracking at the notch tip.

2 MODELING ASSUMPTIONS AND PARAMETER CALIBRATION

The general aim of this work, is to provide a deeper insight into the tensile behaviour and strain localisation processes in thermally pre-damaged concrete. In particular the role of fracture properties has been checked, since in concrete structures subjected to fire they may govern the effects of both the strong thermal gradients and fast hygral transients, namely the macro-cracking and the explosive spalling.

To this purpose, the attention has been focused on the tensile behaviour of the cited lower grade concrete (f_c = 72 MPa), which was investigated through both direct tension tests on notched cylinders (fixed-ends) and indirect tension tests (three point bending) on either unnotched and notched prisms (notch ratio 0.25-0.5).

The basic idea underlying the whole work of numerical modelling which has been performed in this work, is that the same concrete after uniform exposure to high temperature, can be simply modelled as a different homogeneous material, where the effects of the undergone thermal damage are included in the values of its mechanical properties. As a matter of fact, since the material heterogeneity at the meso-level increases due to extensive micro-cracking, a major role in the above said hypothesis is played by the material characteristic length, in the sense of a smeared crack approach, in the framework of which the modelling of the whole set of above quoted tests has been herein pursued.

The "crush-crack" non-local damage model (di Prisco and Mazars, 1996) has been in fact adopted, in an updated formulation (Ferrara, 1998), together with a consistent procedure for the identification of parameters governing the spatial averaging algorithms on which the non-locality of the model rely (Ferrara and di Prisco, 2001).

In this model any fracture process in concrete is regarded as the outcome of three different cracking/failure modes, which can be led to three basic stress states: uniaxial tension and uniaxial and biaxial compression. The model hence requires "constitutive" stress-strain curves under the above mentioned stress states to be assigned.

Skipping over the analytical details of the stress-

strain curves under uni- and biaxial compressive stress states, for which the expressions suggested by CEB-MC90 have been used, it is worth here focusing on the hypotheses underlying the modelling of the tensile "constitutive" behaviour of concrete, which can be summarised as follows:

- the pre-peak behaviour has been described as linear up to $f_t/2$ and, further on, by means of a third order parabola, perfectly joined to the linear elastic branch and attaining the peak with a zero slope at a strain equal to $2f_t/E$;
- the post-peak behaviour has been modelled through a bilinear softening law, the knowledge of which is got once the four following parameters are known: tensile strength f_t, fracture energy G_f, ultimate strain ε_u and material characteristic length *h*.

Furthermore, in order to completely define the bilinear softening curve, a suitable assumption has to be made on the partitioning of the specific volume fracture energy into the areas subtended by the two branches of the softening curve.

The role of the material characteristic length *h* has to be suitably remarked: it allows the transition from the specific surface fracture energy G_f, as determined from the experimental stress-crack opening curves, to the specific volume fracture energy g_f, which is deemed to be dissipated within a crack band width and is regarded as the area subtended by the input stress-strain curve.

In this work f_t, G_f and *h* have been regarded as independent parameters and the ultimate strain has been computed, as a first trial, by adapting the Hordijk's relationship (1991) to a smeared crack context, as $\varepsilon_u = 5.14\, G_f/hf_t$. Furthermore it has been assumed that the area subtended by the first softening branch is equal to 2/3 of the total specific volume fracture energy. As for the value of the characteristic length *h*, it has been assessed, in the experimental program this work refers to, by means of a combined numerical/experimental approach (di Prisco et al., 1999), the results of which have been herein taken as a starting point.

Entering into details, the ratio between the initial slope of the softening tension curves as from direct tension tests on notched cylinders (stress-crack opening) and PIED tests on unnotched prisms (stress-strain) has been experimentally measured and defined as a "first cracking characteristic length" h^I. The material characteristic length *h*, involving all the fracture process identified from the cross examination of the previously quoted couple of tests, has been hence numerically calibrated and turned out to be roughly equal to $2h^I$. The numerical internal length l_c, which is related to the material characteristic length *h*, governs the size of the non-local averaging support (actually equal to 3 l_c); in this work the ratio h/l_c has been taken equal to 7 (Ferrara and di Prisco, 2001).

The reliability of the whole set of modelling hypotheses, which is summarised in Table 2, as far the values of the relevant material properties, has been checked with reference to the undamaged concrete, by modelling both direct tension tests on notched cylinders and three-point bending tests on notched prisms (notch ratio 0.25). Meshes employed for the analyses are shown in Figure 6; for both specimens their symmetry features have been considered in the analyses.

Results are shown in Figures 7,a-b and clearly show a significant overestimation of the peak load in bending, which can be surely connected to the incorrect modelling of the first softening slope in direct tension: both phenomena may depend on an overestimation of the first cracking fracture energy G_{fI}, i.e. the area subtended by the first branch of the softening curve, assumed equal, in these first calibration tests, to 2/3 of the total fracture energy.

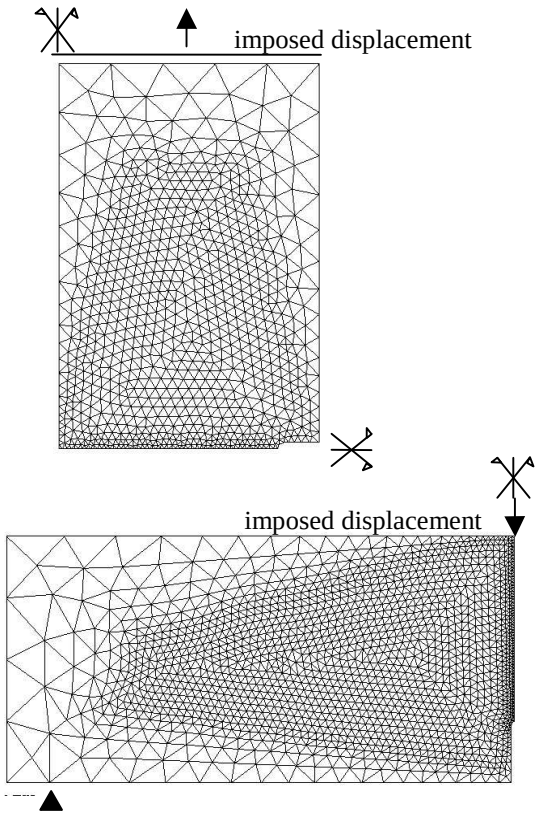

Figure 6: Meshes employed for analyses of direct tension tests and 3-point bending tests on notched beams.

Table 2. Material parameters for calibration analyses on thermally undamaged concrete

	1st case	2nd case	3rd case	4th case
Compressive Strength f_c (MPa)	72			
Young modulus E (GPa)	44.5			
Tensile strength f_t (MPa)	4.45			
Fracture energy G_f (N/mm)	0.277			
characteristic length *h (mm)*	17			
$g_f = G_f/h$ (N/mm^2)	0.016			
$g_{fI} = G_{fI}/h$ (N/mm^2)	***0.012 (2/3 g_f)***	***0.009 (exp.)***	***0.009 (exp.)***	***0.009 (exp.)***
Ultimate strain ε_u	***1.88 e-2***	***9.41 e-2***	***3.76 e-2***	***1.88e-2***

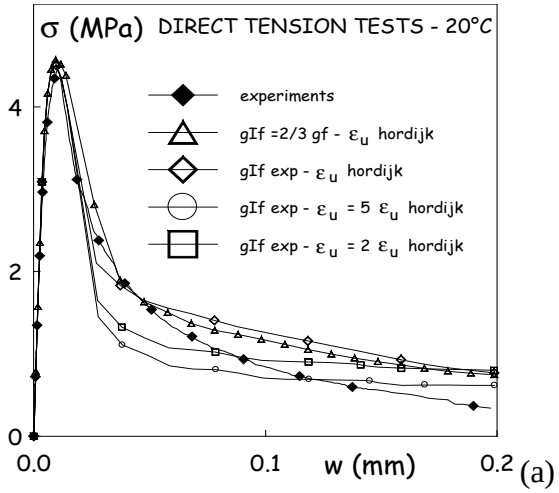

(a)

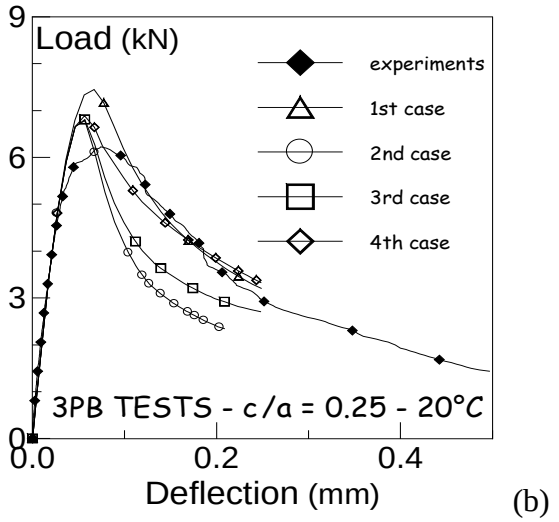

(b)

Figure 7. Parameter calibration on direct (a) and indirect (b) tension tests – thermally undamaged concrete.

It has been then decided to exploit the very detailed corpus of experimental results taking the slope of the first softening branch equal to the one experimentally identified through PIED tests (or, equivalently, to the one from direct tension tests divided by h^I, as before said). Furthermore, a parameter investigation on the role played by the slope of the second softening branch has been performed simply by varying the value of the ultimate tensile strain, at fixed slope of the first softening branch to the above said value. Three different values for the ultimate strain have been considered, namely $\varepsilon_u = 5.14\ G_f/h\ f_t$ and ε_u respectively equal to twice and four times this value (still refer to Table 2 for input values of relevant material parameters).

The results of this further parameter calibration, always performed with reference to direct and indirect tension tests on the undamaged concrete, are shown still in Figure 7 and clearly confirm, as far the modelling hypotheses at issue are dealt with:

- on the one hand the importance of a proper calibration of the slope of the first softening branch of the uniaxial constitutive law, for a correct prediction/reproduction of the peak load in bending;
- the not immediate role of the ultimate strain on a proper modelling of the post-peak behaviour in bending;
- the overestimation of the residual stresses in direct tension, which can be regarded as a sort of inborn feature/drawback of smeared crack approaches, mainly of non-local models, which preserve the continuum hypothesis up to failure, unless an evolutionary characteristic length approach is suitably employed (Mosalam and Paulino, 1997; Ferrara and di Prisco, 2002).

Table 3. Calibrated material properties for concretes at different thermal damage levels

	T = 20°C	T = 250°C	T = 400°C
Compressive strength f_c (MPa)	72	58	26
Young modulus E (GPa)	44.5	26	7.5
tensile strength f_t (MPa)	4.45	3.15	1.20
fracture energy G_f (N/mm)	0.277	0.189	0.253
Characteristic length *h (mm)*	17	33	100
$g_f = G_f/h$ (N/mm^2)	0.016	0.0057	0.0025
g_{fI} (N/mm^2)	***0.009 (exp)***	***0.0045 (exp)***	***0.0016 (exp)***
ultimate strain ε_u	***1.88 e-2***	***9.35 e-3***	***1.08 e-2***

3 NUMERICAL RESULTS: DIRECT AND INDIRECT TENSION

On the basis of previously shown results the whole set of experimental tests has been hence modelled by assuming for concrete in tension an input constitutive law where the slope of the first softening branch directly comes from PIED tests. As for the second branch of the curve, the formula for the ultimate strain value $\varepsilon_u = 5.14\ G_f / h\ f_t$ (which proved to be reliable on undamaged concrete) has been tentatively extended to the whole temperature range. In Table 3 the values of the relevant material parameters for all the investigated cases are summarised.

Results for direct tension tests and for three point bending tests on either unnotched and notched prisms and for the three different chosen significant thermal damage levels (20°C, 250°C and 400 °C) are shown in Figures 8 to 11. For unnotched beams and notched beams with notch ratio equal to 0.5 meshes similar to those shown in Figure 6b have been employed, always analysing half specimen for the sake of its symmetry. The reliability of the previously exposed and calibrated modelling assumptions clearly appears.

In Figure 11 (beams with notch ratio equal to 0.5), both experimental curves have been plotted for the case T = 400°C, instead of the mean one, as in all the other cases. This because of the quite significant experimental scattering, probably due to a quite large initial damage randomly caused by both the higher temperature and the deeper notch. This occurrence is likely to furthermore cast some doubts about the reliability of such a test geometry for the identification of fracture properties in concretes which underwent strong thermal damage.

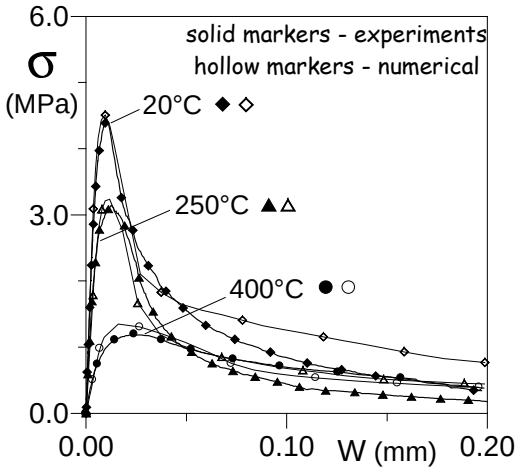

Figure 8. Fixed-end direct tension tests on notched cylinders.

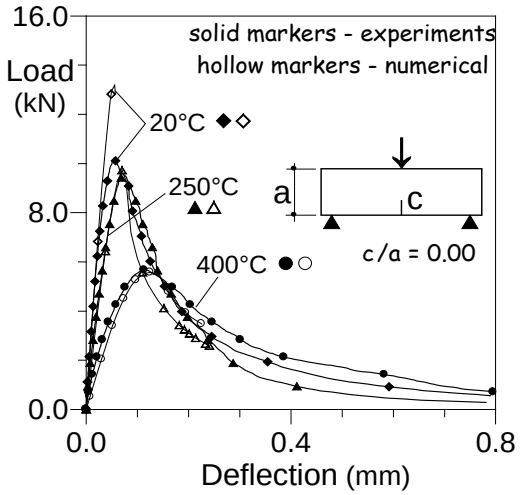

Figure 9. 3-point bending tests on unnotched beams.

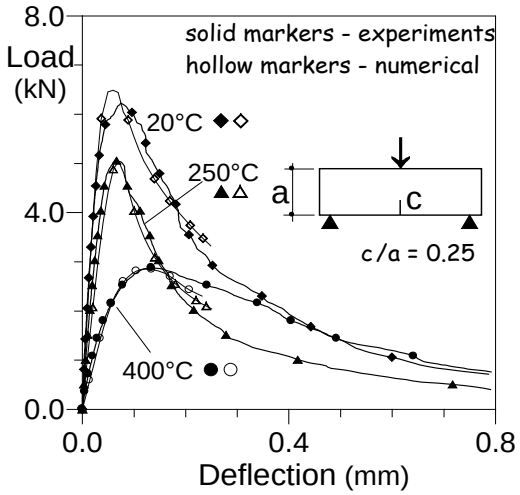

Figure 10. 3-point bending tests on beams with notch ratio 0.25.

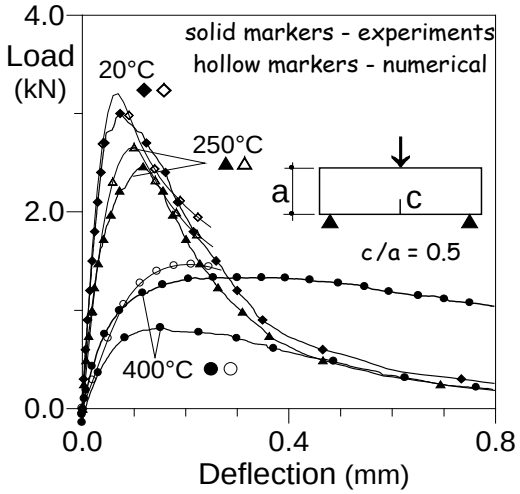

Figure 11. 3- point bending tests on beams with notch ratio 0.5.

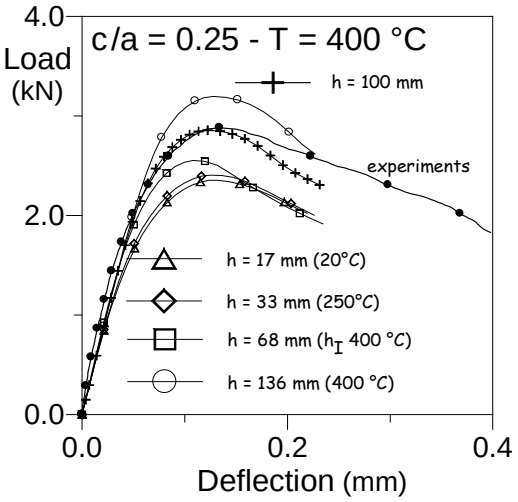

Figure 12. Influence of characteristic length - 3 point bending tests on notched beams (notch ratio 0.25) T = 400 °C.

A sizable overestimation of the peak load has been detected for the unnotched beam made with thermally undamaged concrete. A material sensitivity to a randomly placed defect, which may furthermore affect the specimen symmetry, can be called to explain this fact. A trial analysis has hence been performed in which all the beam has been considered and just beside the symmetry axis, only on one hand, a 5mm x 5mm defect spot has been placed (the "defected" material has tensile strength and fracture energy equal to 20% of the bulk material). The results obtained, as far the peak load is concerned, are reported in Table 4 and confirm the reliability of the above said hypothesis.

The importance of a proper identification of the temperature dependence of the characteristic length h (and hence of the width of the non-local averaging support = 3 l_c = 3/7 h) has been further checked. With reference to three point bending test at 400°C (c/a=0.25), it clearly appears that the sensitivity of the structural response rises as far as the size of the averaging support approaches the ligament length (Figure 12).

4 CHECK ON UNREINFORCED DEEP BEAMS

In order to further check the reliability of the previously calibrated modeling assumptions the case of an unreinforced deep beam (span/depth ratio ≅ 2) has been numerically analyzed, for the three thermal damage levels at issue (20°C, 250°C and 400 °C). The beams were 550 mm long (500 mm span), 275 mm high and 80 mm thick. The modeling has been performed by considering the symmetry of the specimen (Figure 13a).

Table 4. Peak loads for three point bending tests on unnotched beam – thermally undamaged concrete

Experimental	10.2 kN
Numerical symmetric	13.2 kN
Numerical with asymmetric defect	10.7 kN

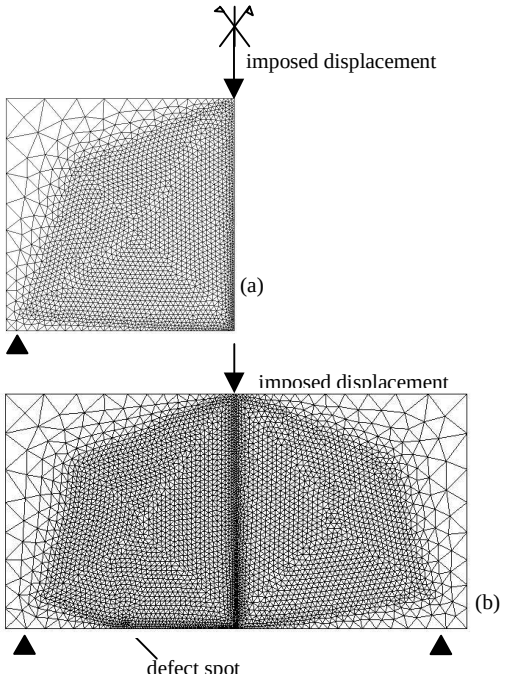

Figure 13. Meshes employed for the analysis of unreinforced deep-beams: symmetric (a) and asymmetric with defect (b).

Since in the experiments a snap-back of the load-deflection response occurred (the control variable was the crack opening displacement at the specimen intrados), the comparison has been performed just with reference to the peak load (no algorithm to control snap-back, such as arc-length, was adopted in the analyses). Results summarized in Table 5 show an overestimation of the maximum load for both T = 20°C and 250°C while a quite good "prediction" is achieved for T = 400 °C. It has to be remarked that it is quite common for these structures to undergo asymmetric failure (Figure 14 - Felicetti et al., 1999) while numerical analyses hypothesized perfect symmetry and hence reproduced a failure featured by a single central crack. This may be called to explain the computed overestimation of the peak load. A trial analysis performed on the thermally undamaged beam by placing, close to the quarter of the beam span, a 5mm x 5mm defect spot (20% strength and fracture energy of the bulk material - see the mesh in Figure 13b) confirmed, as in Table 5, this hypothesis.

Table 5. Peak loads for unreinforced deep beams

	T = 20 °C	T = 250 °C	T = 400 °C
Experimental	45.3 kN	34.2 kN	15.3 kN
Numerical	57.0 kN	43.5 kN	17.0 kN
″ with defect	42.0 kN		

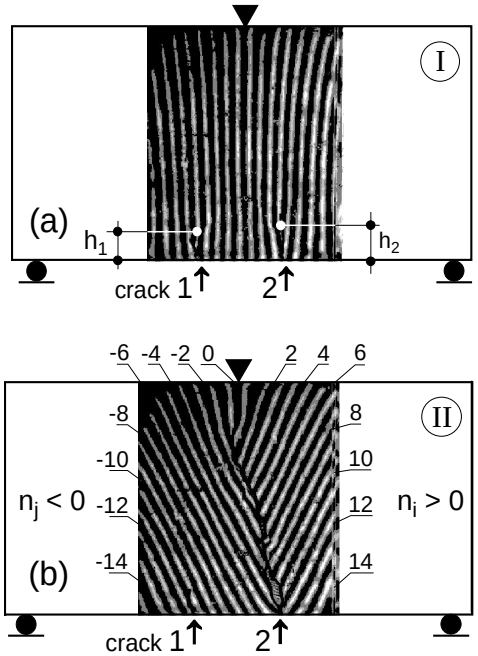

Figure 14. Moiré fringe patterns at peak load P_{max} (a) and at $P_{max}/3$ on the softening branch (b) for an undamaged deep beam.

5. CONCLUDING REMARKS

The residual mode I fracture properties of high performance highly siliceous concretes subjected to thermal damage have been assessed in this paper by means of non-local damage modeling. The basic idea underlying the whole work is that the same concrete after uniform exposure to high temperature, can be simply modelled as a different homogeneous material, where the effects of the undergone thermal damage are included in the values of its mechanical properties.

A suitable calibration of material parameters for thermally undamaged concrete has been first of all performed with reference to both direct tension tests on notched cylinders (fixed ends) and three-point bending tests on notched beams (notch ratio 0.25). This showed the importance of a proper definition of the input tensile constitutive law, mainly of the slope of the first softening branch and secondly of the ultimate strain value.

The reliability of the calibration procedure has been confirmed for the whole temperature range by the analyses of direct tension and indirect tension tests on beams with different notch-ratios. A final check on unnotched specimens (slender and deep beams) showed the sensitivity of the peak load to randomly placed defects, especially in the case of thermally undamaged material. This problem may deserve further investigation concerning the size, position and amount of the defect.

The work confirmed the key role played by the characteristic length on the temperature sensitive behavior of the material. The need of properly identifying the value of the material characteristic length as well as its dependence on the temperature has been pointed out.

REFERENCES

di Prisco, M. & Mazars, J. 1996. Crush-Crack: A non-local damage model for concrete. *Journal of Mechanics of Cohesive and Frictional Materials* 1 (3): 321-347

di Prisco, M., Felicetti, R. & Gambarova, P.G. 1999. On the evaluation of the characteristic length in high strength concrete. *High Strength Concrete*, A. Azizinamini et al. eds., ASCE, Reston, VA, USA: 377-390.

Felicetti R. and Gambarova P.G. 1998a. The effects of high temperature on the residual compressive strength of high-strength siliceous concretes. *ACI Materials Journal*, 95 (4): 395-406.

Felicetti, R. & Gambarova, P.G. 1998b. On the residual tensile properties of high performance siliceous concrete exposed to high temperature. *Intern. Workshop in honor of Z.P. Bazant's 60th anniversary*, Ed. Hermes (Paris): 167-186.

Felicetti R., Gambarova P.G. e Semiglia M. 1999. Residual capacity of HSC thermally damaged deep beams, *ASCE - Journal of Structural Engineering*, 125 (3): 319-327.

Felicetti R., Gambarova P.G., Natali Sora M.P. and Khoury G.A 2000: "Mechanical behaviour of HPC and UHPC in direct tension at high temperature and after cooling", Proceedings 5th Symposium on Fibre-Reinforced Concrete BEFIB 2000, Lyon (France): 749-758.

Ferrara, L. 1998. A contribution to the modelling of mixed-mode fracture and shear transfer in plain and reinforced concrete, *PhD Thesis*, Department of Structural Engineering, Politecnico di Milano, Italy, 245 pp.

Ferrara, L. & di Prisco, M. 2001. Mode I fracture behavior in concrete: non-local damage modeling. *ASCE Journal of Engineering Mechanics* 127(7): 678-692.

Ferrara,L. & di Prisco, M. 2002. An evolutionary internal length approach, *15th ASCE Engineering Mechanics Conference*, Columbia University, New York, NY, USA, (CD Rom).

Hordijk, D. 1991. Local approach to fatigue of concrete, *Ph.D.Thesis*, Delft University of Technology, 1-207.

Mosalam, K.M. & Paulino, G.H. 1997. Evolutionary characteristic length method for smeared cracking finite element models. *Finite elements in analysis and design*, 27: 99-108.

Phan L.T. and Carino N.J. 1998. Review of Mechanical Properties of HSC at Elevated Temperature, *ASCE Journal of Materials in Civil Engineering*, 10 (1): 58-64.

RILEM-Committee 44-PHT 1985, Behaviour of Concrete at High Temperatures. U. Schneider ed., Department of Civil Engineering, Gesamthochschule, Kassel Universität, Kassel (Germany), 122 pp.